COLLABORATIVE PROJECT:
OCEAN-ATMOSPHERE INTERACTION FROM MESO- TO PLANETARY-SCALE: MECHANISMS, PARAMETERIZATION, AND VARIABILITY

FINAL REPORT December 2015 (DE-SC0006821)

This is the final report for the Texas A&M University (TAMU) portion of the project submitted by the PI, R. Saravanan. A comprehensive summary report for the whole collaborative project was submitted by the lead PI, R. Justin Small, from NCAR.

1. Summary

Most climate models are currently run with grid spacings of around 100km, which, with today's computing power, allows for long (up to 1000 year) simulations, or ensembles of simulations to explore climate change and variability. However this grid spacing does not resolve important components of the weather/climate system such as atmospheric fronts and mesoscale systems, and ocean boundary currents and eddies. The overall aim of this project has been to look at the effect of these small-scale features on the weather/climate system using a suite of high and low resolution climate models, idealized models and observations. High-resolution global coupled integrations using CAM/CESM were carried out at NCAR by the lead PI. At TAMU, we have complemented the work at NCAR by analyzing datasets from the high-resolution (28km) CESM integrations (Small et al., 2014) as well as very high resolution (9km, 3km) runs using a coupled regional climate (CRCM) carried out locally (Figure 1).

The main tasks carried out were:

1. Analysis of surface wind in observations and high-resolution CAM/CCSM simulations

2. Development of a feature-tracking algorithm for studying midlatitude air-sea interaction by following oceanic mesoscale eddies and creating composites of the atmospheric response overlying the eddies.

3. Applying the Lagrangian analysis technique in the Gulf Stream region to compare data from observational reanalyses, global CESM coupled simulations, 9km regional coupled simulations and 3km convection-resolving regional coupled simulations.

Our main findings are that oceanic mesoscale eddies influence not just the atmospheric boundary layer above them, but also the lower portions of the free troposphere above the boundary layer. Such a vertical response could have implications for a remote influence of Gulf Stream oceanic eddies on North Atlantic weather patterns through modulation of the storm track, similar to what has been noted in the North Pacific (Ma et al., 2015). The coarse resolution observational reanalyses perhaps underestimate the atmospheric response, but the 28km global model resolution appears to be adequate to capture some, but not all, aspects of the boundary response. The higher resolution regional models show a stronger response in certain fields such as the latent heat flux.

2. Results

2.1 Analysis of surface winds in global and regional simulations

A study comparing results from high-resolution CCSM simulations to regional model simulations has been carried out. The study focused on the analysis of wind power density simulations over the continental U.S., as well as adjoining coastal regions, in existing model runs. Wind power density is an important factor determining the capacity for generating energy from wind. Due to the cubic dependence of power density on wind speed, this is a very sensitive metric for evaluating climate simulations. The global climate models, such as the CCSM, fail to reproduce the fine-scale features seen in the observations. The regional climate simulation using the WRF model does a better job of capturing the wind speed distribution, although it too exhibits significant biases. We focused on three regions over the US with significant wind power potential and analyzed the variability of surface winds in several model runs (Figure 2). The regional climate simulation using the WRF model does a better job of capturing the wind speed distribution as compared to global simulations although it too exhibits significant biases (Figure 3). A poster with preliminary results was presented at the AMS Fourth Conference on Weather, Climate, and the New Energy Economy (Steinweg-Woods and Saravanan, 2013) and a follow-up talk was presented at the AMS Fifth Conference on Weather, Climate, and the New Energy Economy (Steinweg-Woods and Saravanan, 2014).

2.2 Eddy-tracking algorithm for analyzing atmospheric response to mesoscale ocean variability

We have extended the feature-tracking algorithm developed by Faghmous et al. (2012) called 'EddyScan'. Similar to Chelton et al. (2011), it utilizes thresholds of sea level anomaly (SLA) contours to detect closed features. SLA data is chosen as opposed to sea surface temperature (SST) due to the more physical connection SLA has with eddy formation. Utilizing SST data is more difficult due to many possible influences on gradients, such as fronts and other synoptic scale systems. The parameters of the eddy detection algorithm were tuned on observational satellite measurements of SLA, with these same settings used in the coupled model results as well for a standardized comparison between datasets. The output from all model results was regridded to the same grid as the observational data (0.25^{o}x0.25^{o}) before running the detection algorithm. Any eddies detected within a latitude/longitude range too close to land were then removed. An example of the algorithm's detection process can be seen in Figure 4.

2.3 Lagrangian analysis of atmospheric response to ocean eddies in the Gulf Stream region

The response of atmospheric flow to Gulf Stream eddies was explored using the Lagrangian eddy-tracking analysis described above. The analysis was carried out for satellite observations (AVISO SLA; Reynolds' SST; CCMP winds; TRMM precipitation), reanalyses (NCEP CFSR; Year of Tropical Convection), the high resolution CESM run (Small et al., 2014) and two regional coupled model runs using WRF coupled to ROMS with even higher horizontal resolution (9km and 3km; Figure 1). Lagrangian composites were then computed for atmospheric properties like surface windspeed, boundary layer height, and precipitation over

cyclonic and anticyclonic types of eddies. Our results show that CESM reproduces the surface windspeed response to mesoscale eddies seen in observations (Figure 5). If anything, the CESM response appears to be a bit stronger in this Lagrangian analysis than observed. Table 1 shows the coupling coefficients for various quantities, measuring the response per ^{o}C of SST anomaly. For wind speed and rainfall rate, the model coefficients are stronger than the observational estimates, but CESM and WRF have similar values despite differing horizontal resolutions. For latent heat flux, the WRF coupling coefficients are substantially larger than CESM values, indicating resolution does matter. The horizontal spatial structure of the rainfall response to an oceanic eddy shows a downstream shift in the signal relative to the SST maximum (Figure 6). Vertical composites identify a vertical motion signal that indicates that the atmospheric response penetrates above the boundary layer into the free troposphere, up to the 700mb pressure level (Figure 7). Early results from the eddy-tracking analysis were presented at the American Meteorological Society's 19th Conference on Air-Sea Interaction (Steinweg-Woods et al., 2015). Two manuscripts as well as a Ph.D. thesis based on these results are currently in preparation.

3. Dissemination activities supported by the project

3.1 *Presentations*

Steinweg-Woods, J., and R. Saravanan, 2013: Interannual-to-decadal variability of wind power density over the continental US: sensitivity to model resolution and teleconnections. Poster presentation at the *American Meteorological Society's Fourth Conference on Weather, Climate, and the New Energy Economy, Austin, TX, January 2013.*

Steinweg-Woods, J., R. Saravanan, 2014: Wind Resource Assessment Utilizing Time-Averaged Community Earth System Model data. Talk presented at *American Meteorological Society's Fifth Conference on Weather, Climate, and the New Energy Economy, Atlanta, February 2014.*

Steinweg-Woods, J., J.-S. Hsieh, R. Saravanan, and P. Chang, 2015: A Lagrangian view of midlatitude air-sea interaction associated with mesoscale oceanic eddies. Talk presented at the *American Meteorological Society's 19th Conference on Air-Sea Interaction, Phoenix, AZ, January 2015.*

3.2 *Manuscripts in preparation*

Steinweg-Woods, J., 2016: A Lagrangian view of midlatitude air-sea interaction associated with mesoscale oceanic eddies. Ph.D. Thesis, *Texas A&M University*

Steinweg-Woods, J., J.-S. Hsieh, R. Saravanan, and P. Chang, 2016: The near-surface atmospheric response to mesoscale ocean eddies in the Gulf Stream separation region

Steinweg-Woods, J., J.-S. Hsieh, R. Saravanan, and P. Chang, 2016: The vertical structure of the atmospheric response to mesoscale ocean eddies in the Gulf Stream separation region

6. Other References

Chelton D.B., Schlax, M.G., and Samelson, R.M., 2011: Global observations of nonlinear mesoscale eddies. *Progress in Oceanography* 91, 167–216.

Faghmous, J.H.; Styles, L., Mithal, V., Boriah, S., Liess, S., Kumar, V., Vikebo, F., dos Santos Mesquita, M., 2012: EddyScan: A physically consistent ocean eddy monitoring application, *2012 Conference on Intelligent Data Understanding* (CIDU), 96-103.

Ma, X., P. Chang, R. Saravanan, R. Montuoro, J.-S. Hsieh, D. Wu, X. Lin, L. Wu, Z. Jing, 2015: Distant Influence of Kuroshio Eddies on North Pacific Weather Patterns? *Nature Scientific Reports* 5, 17785; doi: 10.1038/srep17785

Small, R. J., and co-authors, 2014: A new synoptic scale resolving global climate simulation using the Community Earth System Model, *J. Adv. Model. Earth Syst.*, 6, 1065–1094, doi:10.1002/2014MS000363.

7. Tables and Figures

Variable Type	Observations	CESM	WRF 9km	WRF 3km
Wind Speed (m s^{-1} $°C^{-1}$)	0.17	0.28	0.20	0.22
Rainfall Rate (mm day^{-1} $°C^{-1}$)	0.10	0.14	*0.18*	*0.17*
Cloud Fraction (% $°C^{-1}$)	1.02			
Surface Solar Flux (W m^{-2} $°C^{-1}$)		-1.25	-0.42	-0.74
Latent Heat Flux (W m^{-2} $°C^{-1}$)		28.21	38.52	38.62
Boundary Layer Height (m $°C^{-1}$)			37.16	38.36

Table 1. Coupling coefficients between SST anomalies and anomalies of the variable type listed. Values in italics were not a statistically significant linear fit in the F-test (p-values $>$ 0.01).

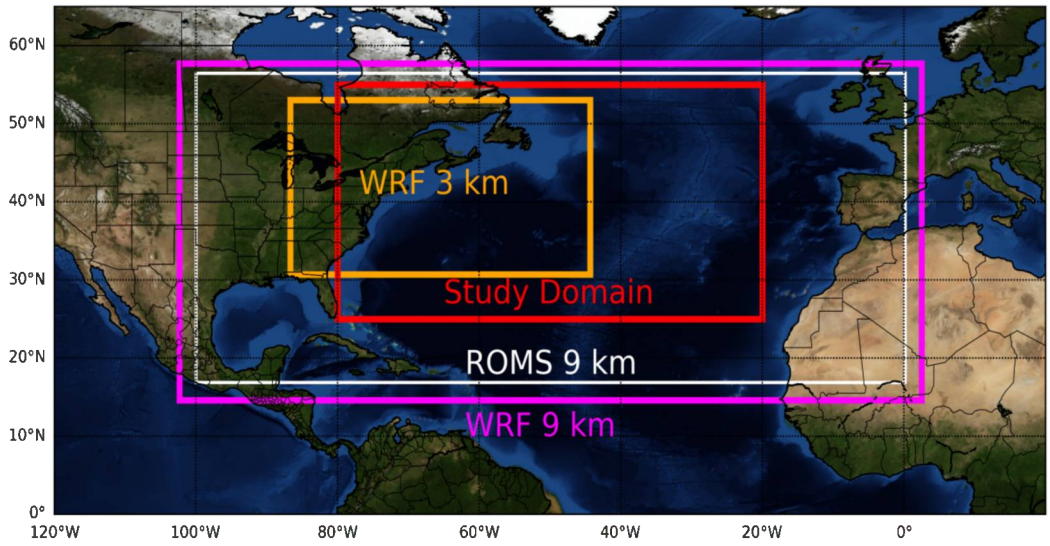

Figure 1. The domains of the WRF 9km, ROMS 9km, and WRF 3km nest are shown. The domain used for the Lagrangian eddy-tracking analysis is shown as the red box.

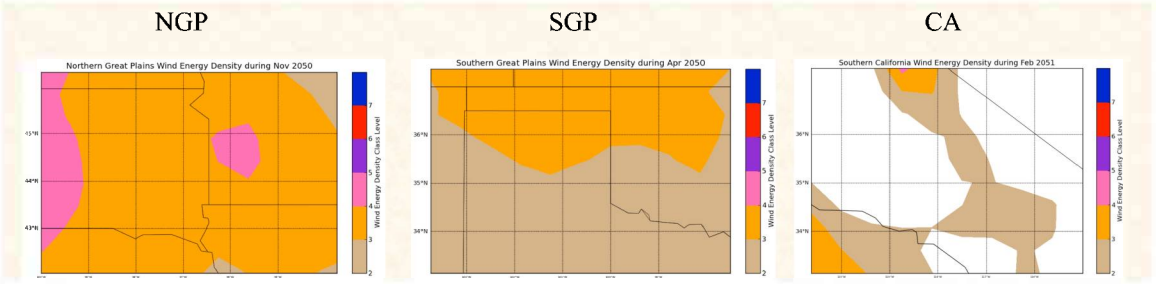

Figure 2: Wind power density estimated from a CCSM (Community Climate System Model) integration (40.007b) for the years 2050-2051 in a future climate assessment scenario for the Northern great Plains (NGP), Southern Great Plains (SGP) and California (CA). Note that the model resolution of 62.75 km is not adequate to resolve topographical features, especially in CA.

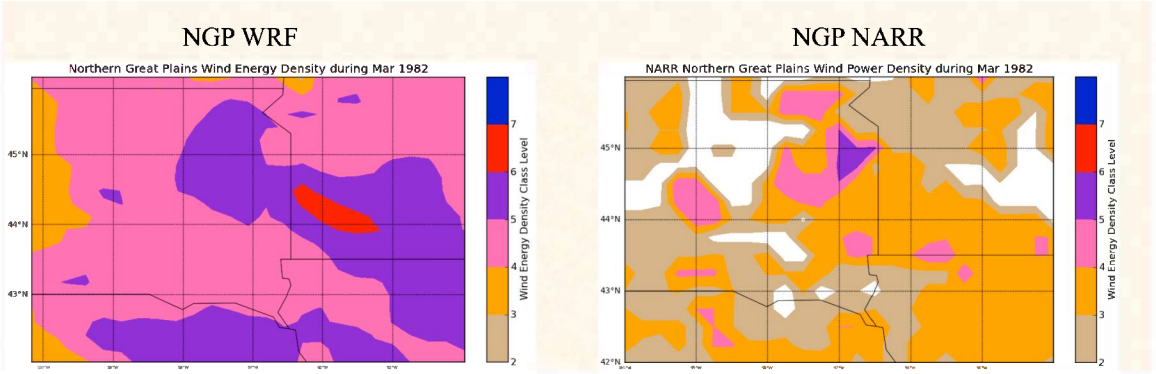

Figure 3: Comparing wind power density over the NGP region for a 27-km WRF simulation (left) and the North American Regional Reanalysis (right).

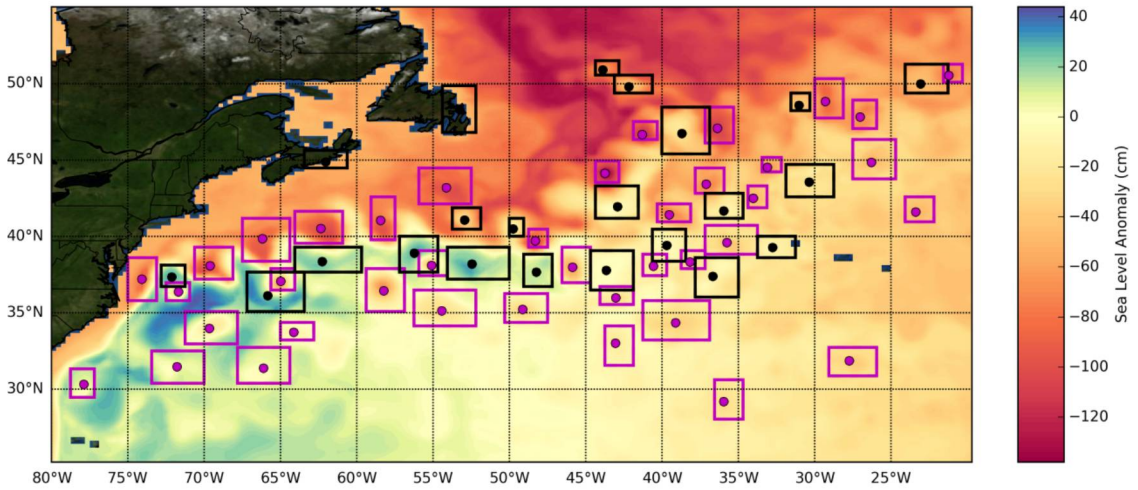

Figure 4. An example of the eddy detection algorithm from sea level anomaly data on January 1, 2006 inside the study domain. Anticyclonic eddies containing positive sea level anomalies are highlighted with black boxes, while cyclonic eddies with negative sea level anomalies are highlighted with magenta boxes. The detected eddy center is indicated by a small circle inside each box. Eddies erroneously detected too close to land were removed in the final calculations.

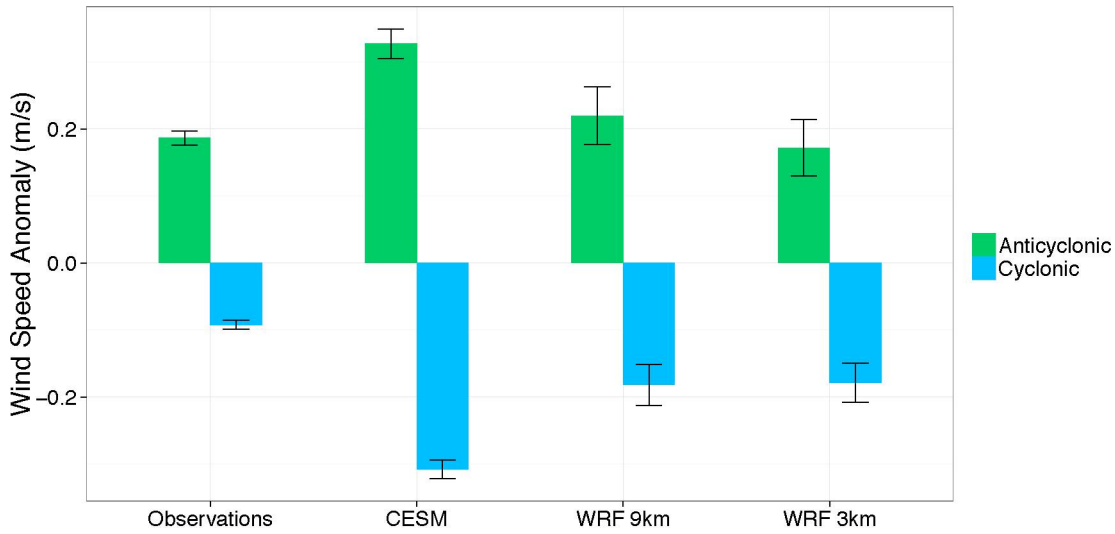

Figure 5. Results from Lagrangian composite analysis of the wintertime surface windspeed response to cyclonic and anticyclonic eddies in the Gulf Stream separation region, comparing scatterometer observations to the CESM control integration and two regional coupled model integration using ROMS and WRF (at 9km and 3km horizontal resolution respectively).

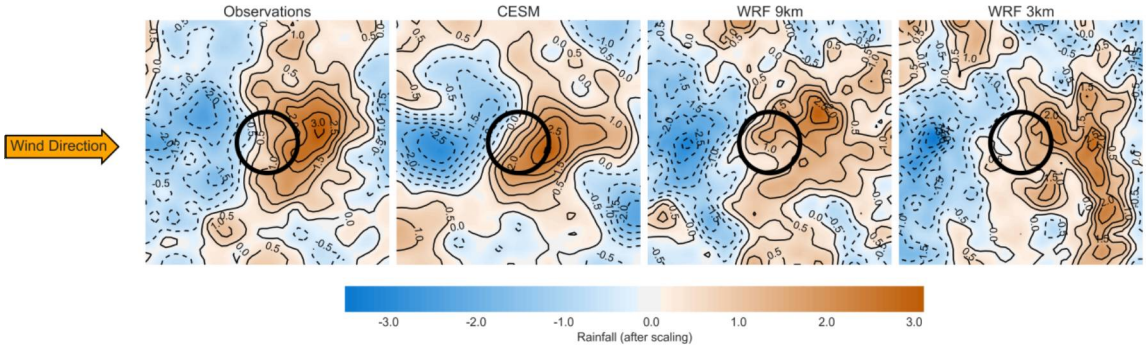

Figure 6. Difference between warm core and cold core composites for rainfall rate. Due to differing magnitudes between observations and model results, the composites are normalized to a mean of zero and standard deviation of one for better visual comparison.

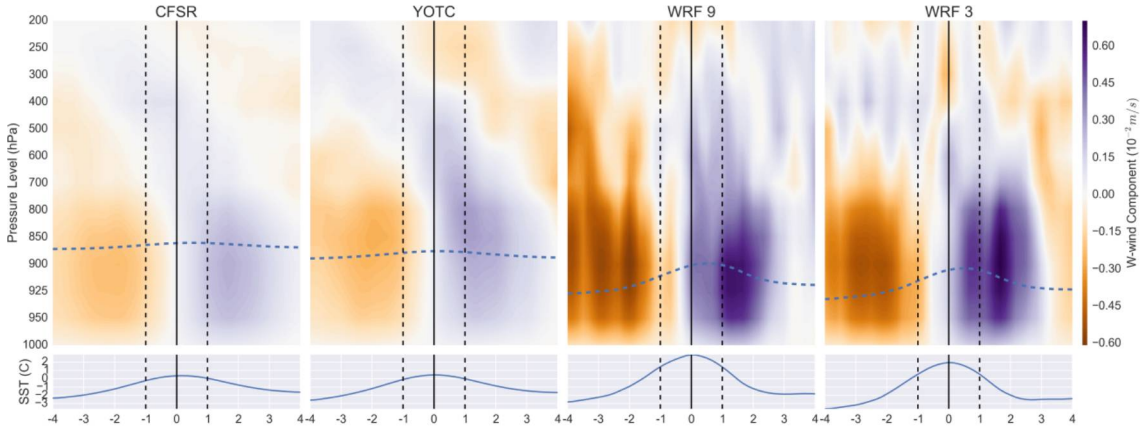

Figure 7. Vertical composites of the vertical component of wind in response to the eddies. Zonal means have been subtracted in each vertical layer, and the difference between eddy types is shown (warm core minus cold core). The dotted blue line represents the difference between the boundary layer heights of each eddy type, which has been added to the average between the two in order to plot the boundary layer's position relative to the anomalies. The difference between eddy types for SST along a central chord is also shown at the bottom of the plot. The vertical dotted lines represent the outer edges of a single scaled eddy radius, with x-axis indicating the number of eddy radii outward from the center at the bottom of each subplot.